

We are IntechOpen, the world's leading publisher of Open Access books Built by scientists, for scientists

6,900

Open access books available

186,000

International authors and editors

200M

Downloads

Our authors are among the

154

Countries delivered to

TOP 1%

most cited scientists

12.2%

Contributors from top 500 universities



WEB OF SCIENCE™

Selection of our books indexed in the Book Citation Index
in Web of Science™ Core Collection (BKCI)

Interested in publishing with us?
Contact book.department@intechopen.com

Numbers displayed above are based on latest data collected.
For more information visit www.intechopen.com



Fabrication of Surfaces with Bimodal Roughness Through Polyelectrolyte/Colloid Assembly

Christine C. Dupont-Gillain*, Cristèle J. Nonckreman,
Yasmine Adriaensen and Paul G. Rouxhet

*Institute of Condensed Matter and Nanosciences - Bio & Soft Matter,
Université Catholique de Louvain
Belgium*

1. Introduction

From bioengineering to optics and electronics, a great deal of work has been conducted on the development of new materials with structured surfaces. A large range of methods has been used, such as plasma etching, electron beam and colloidal lithography (Denis et al., 2002), electrical deposition (Yang et al., 2009), phase separation (Dekeyser et al., 2004) and polyelectrolyte assembly in order to produce structured surfaces (Agheli et al., 2006). The combination of different methods is also more and more explored. Schaak et al. (2004) described a simple approach to achieve colloidal assembly on a patterned template obtained by lithography.

Densely packed layers of colloidal particles can be produced by lifting a substrate vertically from a suspension (Fustin et al., 2004; Li J. et al., 2007) or by spin coating (Yang et al., 2009). Colloidal lithography utilizes the ability of particles to adhere on oppositely charged surfaces (Johnson & Lenhoff, 1996; Hanarp et al., 2001, 2003)), possibly using surface modification by inorganic or organic polyelectrolytes. The surface coverage is influenced by several factors: ionic strength, particle size and time. The adhesion of microbial cells on various substrates was also achieved by surface treatments with inorganic or organic polycations (Changui et al., 1987; Van haecht et al., 1985) or with positively charged colloidal particles (Boonaert et al., 2002). A review on colloidal lithography and biological applications was published recently (Wood, 2007).

Adsorption of polyelectrolytes is influenced by ionic strength, pH and the polyelectrolyte characteristics (molecular mass, charge density) (Lindquist & Stratton, 1976; Davies et al., 1989; Choi & Rubner, 2005). At low ionic strength, highly charged polyelectrolytes adopt extended conformations and are fairly rigid due to the strong repulsion between charged units. The maximum adsorbed amount and the adsorbed layer thickness do not vary markedly according to molecular weight. As the salt concentration is increased and the electrostatic intrachain repulsion is decreased, the polyelectrolyte becomes more coiled. In this case, the maximum amount adsorbed (expressed in mass) increases as a function of molecular weight (Roberts, 1996; Lafuma, 1996; Claesson et al., 2005; Boonaert et al., 1999).

Build up of polyelectrolyte films may be achieved using layer-by-layer assembly through alternating adsorption of oppositely charged polyelectrolytes (Decher & Hong, 1991).

Polyethyleneimine (PEI), polyallylamine (PAH), poly-L-lysine (PLL) and polydiallyldimethylammonium chloride (PDDA) are common polycations used for multiple layer formation with polyanions such as polystyrene sulfonate (PSS) (Bertrand et al., 2000). Layer-by-layer assembly of polyelectrolytes has been combined with the use of colloidal particles. For instance, a film was made on silicon wafers precoated with thermally evaporated titanium, by adsorption of PDDA, followed by adsorption of PSS, followed by treatment with an aluminium chloride hydroxide solution (Hanarp et al., 2001, 2003). In another study, chemically patterned surfaces made by self-assembled monolayers (SAMs) were covered with a polyelectrolyte multilayer film, before adhesion of SiO₂ silica particles or functionalized polystyrene latex particles (Chen et al., 2000). While a polyelectrolyte layer may provide a strong bond to colloidal particles, the drying process applied after particle adhesion may be crucial to obtain a regular and homogeneous monolayer (Hanarp et al., 2003).

Structured hydrophobic surfaces have gained increasing interest because the roughness amplifies the hydrophobicity (Wenzel, 1936). This is exemplified by the Lotus effect, in which a dual size roughness seems to be important (Barthlott & Neinhuis, 1997; Patankar, 2004). Raspberry-like surface morphologies were created in different ways : styrene polymerization (Perro et al., 2006; Reculosa et al., 2002) or gold sputtering (Xiu et al., 2006) on silica particles , controlled aggregation of different surface-functionalized silica particles (Ming et al., 2005) or direct electrochemical synthesis of gold microaggregates (Li Z. et al., 2007) and immobilization on a specific substrate.

In this paper, we prepare surfaces covered with a homogeneous monolayer of colloidal particles, using adhesion of negatively charged polystyrene latex beads on a polycation-precoated glass substrate. The method is then extended to prepare surfaces presenting a bimodal roughness, by using latex particles of different sizes. The influence of substrate surface roughness on the behavior of mammalian cells has been of great concern in the last years (Nonckreman et al., 2010). Therefore, the stability of fabricated samples is tested in phosphate buffer saline (PBS), which simulates the pH and ionic strength of biological fluids. Note that here, the term "colloid" is used with the restrictive sense of lyophobic colloidal particle, and thus distinguished from polyelectrolytes.

2. Materials and methods

2.1 Materials

Glass substrates were microscope coverslips (12 mm diameter, Menzel-Gläzer, Germany). Polyethyleneimine solution (PEI, $M_w = 750\,000$), polyallylamine hydrochloride (PAH, $M_w \sim 70\,000$), poly-L-lysine hydrobromide (PLL, $M_w = 70\,000$ to $150\,000$), poly(diallyldimethylammonium chloride) solution (IPDDA, $M_w < 100\,000$; hPPDA, $M_w = 400\,000$ to $500\,000$) were purchased from Sigma-Aldrich (St. Louis, MO, USA). Negatively charged polystyrene particles with two different sizes (sulfate latex, 65 ± 6 nm, 470 ± 12 nm) were purchased from Interfacial Dynamic Corporation (IDC, Tualatin, OR, USA). The composition of the phosphate buffer saline solution (PBS) was as follows: 137 mM NaCl, 6.4 mM KH₂PO₄, 2.68 mM KCl, 8 mM Na₂HPO₄; adjusted to pH 7.4 with 1M NaOH.

2.2 Sample preparation

Figure 1 presents the different steps of sample preparation, from the glass substrate to surfaces with bimodal roughness.

2.2.1 Glass substrate conditioning

The glass coverslips were cleaned by overnight immersion in sulfochromic solution and rinsed with water, prior to polycation adsorption (Figure 1a). The pH and ionic strength (I) of the polycation solution were adjusted with NaOH and HCl, and NaCl, respectively. The polycation solution (1 ml) was poured into the wells of a tissue culture plate (Falcon, Becton Dickinson, Belgium, Ref. 353226), where the glass coverslips had been placed earlier, and was left in contact with the substrate for at least 2 h. Unless stated otherwise, the polycation solution was 10^{-5} M at pH 11 and I 10^{-2} M. The samples were rinsed by 6 successive dilutions to avoid exposure to air. Each rinsing step was performed by adding 2 ml of deionized water (produced by a Milli-Q plus system from Millipore, Molsheim, France), stirring gently, and removing 2 ml of liquid. They were then dried under a gentle nitrogen flow (Figure 1b).

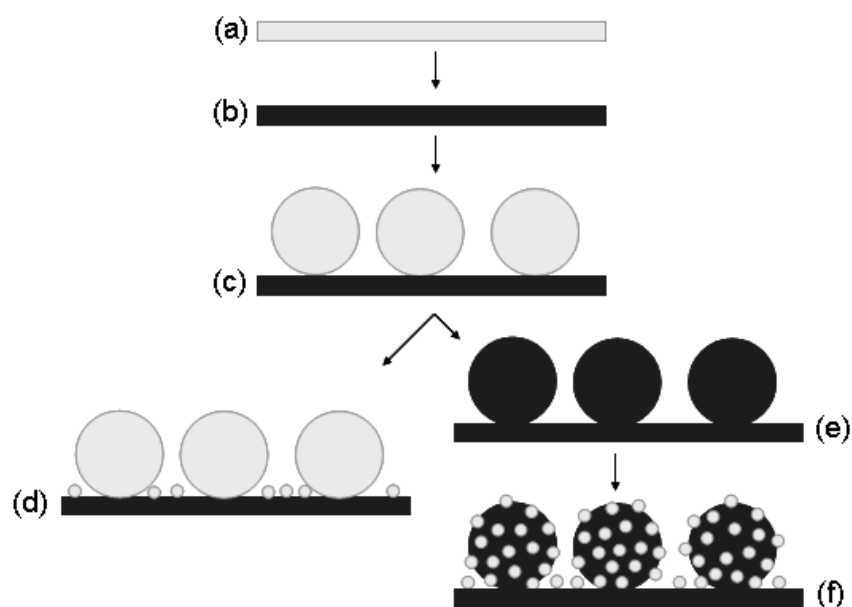


Fig. 1. Schematic representation of the steps used for sample fabrication. Glass substrate (a), polycation-conditioned glass substrate (b), substrate with a layer of adhering particles (c), surface with bimodal I roughness (d), substrate with a layer of adhering particles conditioned with the polycation (e), surface with bimodal II roughness (f).

2.2.2 Adhesion of a single colloid layer

Polycation-conditioned substrates were placed horizontally into wells of another culture plate. 1 ml of a suspension of the desired concentration, pH and ionic strength was poured into the wells and left in contact with the substrate for at least 3 h (Figure 1c). Unless stated otherwise, the procedure used for rinsing and drying the samples was performed as follows: rinsing 3 times with water and 3 times with isopropanol and drying overnight in air. The samples were rinsed by successive dilutions as detailed in the preceding paragraph. After the last rinsing, as much as possible of the solution was removed with a pipette.

2.2.3 Surfaces with bimodal I roughness

1 ml of a 0.1 % suspension of 470 nm particles was poured into the wells containing glass substrates conditioned with PAH (10^{-5} M, pH=11, I= 10^{-2} M) (Figure 1b), placed in horizontal

position, and left in contact with the substrate for at least 3 h (Figure 1c). A suspension of 65 nm particles was then added to obtain a final concentration of 0.1 %, and the system was gently stirred and left resting for 1 more hour (Figure 1d). The samples were rinsed and dried using the same procedure as described for adhesion of a single colloid layer.

2.2.4 Surfaces with bimodal II roughness

Substrates with adhering 470 nm particles (Figure 1c), rinsed and dried, were again conditioned with PAH (10^{-5} M, pH=7, I= 10^{-3} M) (Figure 1e), rinsed with water then with isopropanol and dried, as described for the adhesion of a single colloid layer. These samples were then placed horizontally in wells of another culture plate. 1ml of a 0.1% suspension of 65 nm particles was poured into wells and left in contact with the substrate for at least 2 h (Figure 1f). The samples were rinsed and dried using the same procedure as described for adhesion of a single colloid layer.

2.3 Surface characterization

The samples were examined by scanning electron microscopy (SEM) using a high resolution Digital Scanning microscope 982 Gemini (Leo Electron Microscopy, UK) operating at 1 or 2 kV, without any metal coating. SEM images of substrates covered with a monolayer of adhering particles were analyzed after image processing with Adobe Photoshop (version 8). In this way, the white rings defining latex particles were extracted and intensified in order to draw circles for digital processing. The images were binarized and the circles were filled before measurements (Visilog, version 6). A minimum of 500 particles was counted on more than 4 images with 10 000x magnification. The degree of particle coverage was measured as the area of particles divided by the total area. Manual counting was also performed on at least 3 images with 10 000x or 20 000x magnification of each sample. Regarding surfaces with bimodal roughness, no image processing was found suitable for extracting colloidal particles from the background. Manual counting of the 470 nm particles only was performed on at least 4 images.

The surface chemical analysis by X-ray photoelectron spectroscopy (XPS) was performed using a Kratos Axis Ultra Spectrometer (Kratos Analytical, UK) equipped with a monochromatized aluminium X-ray source (powered at 10 mA and 15 kV) and eight channeltrons detector. Charge stabilization was achieved using an electron source (filament current set at 1.9 A, bias -1.1 eV) mounted coaxial to the lens column and a charge balance plate (voltage set at -2.3 V). The rectangular analyzed area was about 0.7 mm \times 0.3 mm. For recording individual peaks, the pass energy was set at 40 eV. In these conditions, the full width at half maximum (FWHM) of the Ag 3d_{5/2} peak was about 0.9 eV. The pressure in the analysis chamber was around 10^{-6} Pa. The following sequence of spectra was recorded: survey spectrum, C 1s, O 1s, N 1s, Si 2p, Cl 2p, B 1s, Na 1s, Zn 2p, Ti 2p, Al 2p, S 2p and C 1s again to check the stability of charge compensation and the absence of sample degradation as a function of time. The binding energy scale was set by fixing the C 1s component due to carbon only bound to carbon and hydrogen at 284.8 eV. The data analysis was performed with the CasaXPS program (Casa Software, UK). Molar concentration ratios were calculated using peak areas normalized on the basis of the acquisition parameters, sensitivity factors, and transmission function provided by the manufacturer. Angle-resolved XPS analyses were performed by using angles between the normal to the sample surface and the direction of photoelectron collection, ϕ , equal to 0°, 45° and 60°.

The streaming potential was determined at 20°C with an instrument purchased from the Department of Physical and Colloid Chemistry (Agricultural University, Wageningen, The Netherlands) (Elgersma et al., 1992) using glass microscope slides from Marienfeld (7.6 x 2.6 cm²; Lauda-Königshofen, Germany). Two plates of the samples to characterize (clean glass, PAH-conditioned glass) were assembled to make a 100 μm-thick chamber. A solution of 0.01M KNO₃ was forced through these two plates. The difference of potential measured at the entrance and the exit of the chamber was used to compute the zeta potential of the substrate (Rouxhet et al., 1993).

3. Results and discussion

3.1 Surface conditioning with PAH

The choice of pH = 11 for PAH adsorption was inspired by the following considerations. The pK_a of ethyl ammonium is 10.6. The apparent pK_a of the PAH used here is 8.7 in water and 9.3 in 0.5 M NaCl (Petrov et al., 2003; Choi and Rubner, 2005); however it is expected to be appreciably higher after adsorption by a negatively charged surface (Tagliazucchi et al., 2008). Conditions of low degree of protonation were chosen in order to allow adsorption of a thick layer. The adsorbed amount was indeed reported to be higher for polymers with low and intermediate cationicities, such as PAH or PLL compared to PEI, and to increase with the molecular mass (Roberts, 1996; Lafuma, 1996), owing to a more coiled conformation. Highly charged polycations, such as PEI, form flat adsorbed layers at low ionic strength (Claesson et al., 2005) and the adsorbed amount increases with pH (Meszaros, 2004).

The surface chemical composition of glass and glass conditioned with PAH (3 independent sets of results) is presented in Table 1. Non-conditioned glass showed the expected organic contamination and a low concentration of nitrogen. In addition, low concentrations of potassium (1-2 %), boron (2-3 %), sodium (1-1.5 %), and traces (< 1 %) of zinc, titanium and aluminium were found. As the analyzed depth decreased (increase of ϕ), the C/Si concentration ratio increased as expected, but N/Si did not vary significantly and N/C decreased. This indicates that nitrogen is associated with the glass matrix or the glass surface and not with the organic contaminants.

After PAH conditioning, polycation adsorption was evidenced by the increase of carbon and nitrogen concentrations and the decrease of silicon and oxygen concentrations. The N_{1s} peak showed components at 401.5 eV and 399.3 eV due to protonated and non protonated nitrogen, respectively. As the analyzed depth decreased (higher ϕ), the apparent concentration of carbon and nitrogen increased as expected, the N/C ratio remained constant, but the proportion of protonated nitrogen decreased appreciably.

The N/C ratio of about 0.14 must be compared with the value of 0.33 expected for pure PAH. This difference may not be due to an orientation of the polymer segments at the surface, given the structure of the repeat unit [-CH₂-CH(-NH-CH₃)-] and the analyzed depth. It is attributed to the simultaneous presence at the surface of PAH and organic contaminants (Caillou et al., 2008). As the N/C ratio does not vary with ϕ , the adsorbed organic layer appears to be a mere mixture, with no preferential accumulation of a component at the outermost surface. In an alternative way, the elemental composition of the adsorbed layer may be estimated by the difference of nitrogen concentration before and after PAH conditioning ratioed to the total carbon concentration, which provides a N/C ratio of 0.11. The adventitious contaminants observed on silica, which showed the same C1s peak shape as that observed here on glass, were modeled by the generic formula C₁₅H₂₈O₄

(Gerin et al., 1995). According to a N/C ratio of 0.11, the adsorbed layer obtained after PAH conditioning would be 33 wt% PAH (density 1.04 g/m³) and 67 wt% C₁₅H₂₈O₄ (density of 0.9 g/cm³).

Substrate	φ	Concentration (Mole fraction, in %)					Concentration ratios		
		C	O	Si	N	S	C/Si	N/C	N ⁺ /N _{tot}
Glass coverslips									
sample 1	0°	12.6	57.2	22.8	0.6	- ^a	0.55	0.05	0.47
	45°	15.6	58.4	19.7	0.4	- ^a	0.79	0.03	0.37
	60°	20.5	56.5	18.0	0.4	- ^a	1.14	0.02	0.33
sample 2	0°	10.1	59.4	24.9	0.9	- ^a	0.41	0.09	- ^b
	60°	16.5	59.6	20.1	0.8	- ^a	0.82	0.05	- ^b
sample 3	0°	11.9	57.7	23.6	0.9	- ^a	0.50	0.07	0.46
PAH pre-coated glass									
sample 4	0°	24.1	46.6	18.6	3.5	- ^a	1.30	0.15	0.31
	45°	31.9	43.3	14.3	4.8	- ^a	2.23	0.15	0.18
	60°	42.5	36.9	11.3	5.6	- ^a	3.76	0.13	0.12
sample 5	0°	22.8	48.5	19.5	3.4	- ^a	1.17	0.15	- ^b
	60°	37.6	40.9	12.5	5.2	- ^a	3.01	0.14	- ^b
sample 6	0°	30.4	42.5	18.6	4.5	- ^a	1.63	0.15	0.49
PAH pre-coated glass with adherent colloidal particles									
sample 7	0°	64.1	21.8	8.1	1.6	0.3	7.91	0.02	0.38
(470 nm)									
sample 8	0°	41.1	38.0	13.9	2.7	0.2	2.96	0.06	- ^b
(470 nm)									
sample 9	0°	52.2	30.4	11.3	2.7	0.4	4.62	0.05	- ^b
(65 nm)									

Table 1. Surface chemical composition determined by XPS (mole fraction with respect to all elements excluding hydrogen) at different photoelectron collection angles φ .

In order to evaluate the thickness of the organic adlayer, the experimental C/Si ratios were compared with ratios computed by considering a layer of constant thickness (t) on top of glass and using equation 1:

$$\frac{C}{Si} = \frac{i_{Si} \sigma_C \lambda_C^{ad} C_C^{ad} [1 - \exp(-t/\lambda_C^{ad} \cos \varphi)]}{i_N \sigma_{Si} [\lambda_{Si}^{su} C_{Si}^{su} \exp(-t/\lambda_{Si}^{ad} \cos \varphi)]} \quad (1)$$

where i_{Si} and i_N are the relative sensitivity factors provided by the manufacturer for Si (0.328) and C (0.278); σ_{Si} and σ_N are the photoionization cross sections for Si (0.817) and C

(1.000). The superscripts ad and su designate the adsorbed overlayer and the substrate, respectively. The concentrations C are: $C_C^{\text{ad}} = 49.6 \text{ mmol/cm}^3$ for contamination layer deposited on glass; $C_C^{\text{ad}} = 46.9 \text{ mmol/cm}^3$ for the layer made by a mixture of 67 % contaminants and 33 % PAH ($N/C = 0.11$); $C_{\text{Si}}^{\text{su}} = 39 \text{ mmol/cm}^3$ for Si in glass (considering that Si concentration in glass is about 90 % of that in pure SiO_2 ; density of 2.6 g/cm^3). The electron inelastic mean free paths were calculated according to Tanuma et al. (1997) with an energy gap of 7 eV: $\lambda_C^{\text{ad}} = 3.9 \text{ nm}$, $\lambda_{\text{Si}}^{\text{ad}} = 3.6 \text{ nm}$, $\lambda_C^{\text{ad}} = 4.4 \text{ nm}$. Figure 2 presents plots of C/Si molar ratios computed using different values of t , as a function of ϕ . The curves are only slightly different if a N/C ratio of 0.14 is considered. Comparison with the experimental data indicates that the organic layer adsorbed after conditioning is about 3 nm, which is about 3 times thicker than the contamination layer. This does not fit closely the apparent proportions of contaminants and PAH in a homogeneous adlayer. Such approach cannot be exploited further owing to the simplicity of the model (homogeneous, flat and compact adlayer) and limited data accuracy. However it indicates that the organic adlayer obtained after conditioning has a thickness of about 3 nm and that PAH coexists with contaminants. The latter may adsorb from the surrounding atmosphere between sulfochromic cleaning and PAH conditioning or after conditioning.

The degree of protonation of PAH in a solution at pH 11 is less than 10 %. The XPS spectra recorded after PAH conditioning (Table 1) gave values of 31 and 49 % for the degree of nitrogen protonation at a photoelectron collection angle $\phi = 0^\circ$. This is in agreement with expectations regarding the effect of local potential on protonation and with data indicating that the apparent pK_a of PAH may be appreciably increased on a negatively charged surface (Tagliacruzchi et al., 2008).

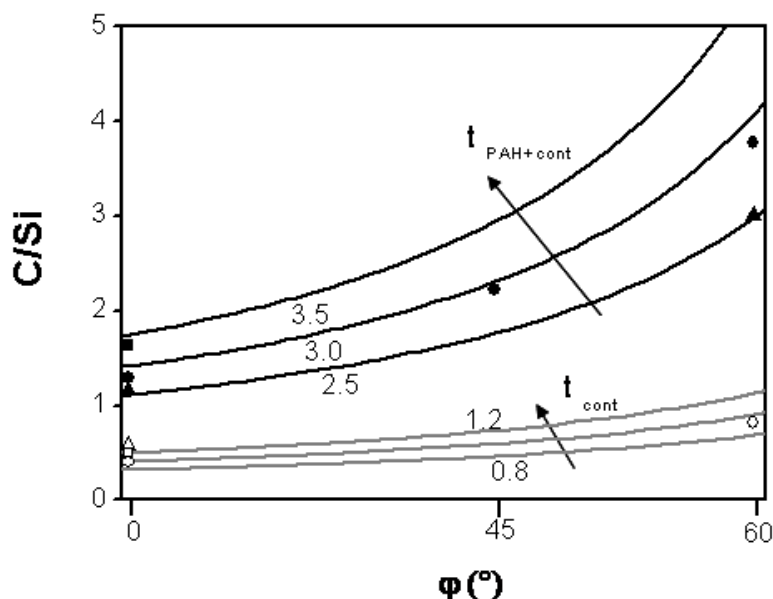


Fig. 2. Plot of computed C/Si molar concentration ratios vs the angle ϕ of photoelectron collection, for non-conditioned glass with a 0.8, 1.0, 1.2 nm thick (t_{cont}) contamination layer, and for PAH-conditioned glass with a 2.5, 3.0 and 3.5 nm thick ($t_{\text{PAH+cont}}$) adlayer made of PAH and contamination. Experimental data for glass (open symbols) and for PAH-conditioned glass (dark symbols). Circles: samples 1 and 4, triangles: samples 2 and 5, squares: samples 3 and 6 (see Table 1).

Figure 3 presents the variation of the zeta potential of glass and of PAH-conditioned glass as a function of pH (in 0.01 M KNO_3). As expected, the glass substrate was found to be negatively charged above pH 2. After polycation adsorption, the zeta potential became less negative, but did not reach positive values. It appears (Figure 3) that adsorbed PAH is shielding the negative charge of glass surface but is not reversing the surface charge. This is in contrast with data reported for substrates such as mica and titanium oxide (Adamczyk et al., 2006, 2007) and is attributed to the fact that here the samples were dried between adsorption and streaming potential measurement, which provoked irreversible shrinkage of the adsorbed layer. It may be related to the decrease of the degree of nitrogen protonation as ϕ increased (Table 1), revealing that it is much higher for segments in close contact with the glass surface. Note that drying after adsorption was a choice made in the context of a fabrication process.

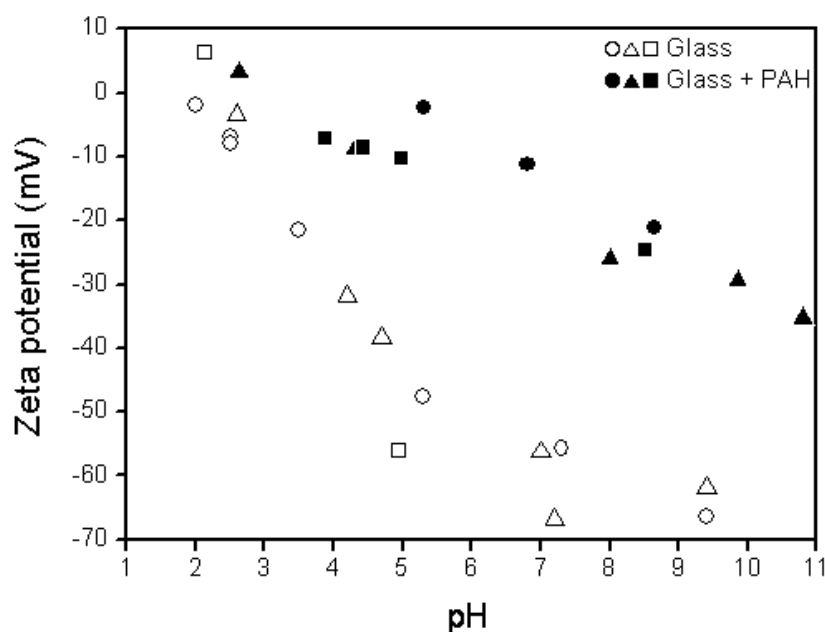


Fig. 3. Zeta potential (mV) of glass (open symbols) and PAH-conditioned glass (dark symbols) as a function of pH in 0.01 M KNO_3 . Three experiments were performed on samples prepared independently.

3.2 Nanostructured surfaces with monomodal roughness

Figure 4a shows representative micrographs of samples prepared with substrates conditioned as described above (PAH 10^{-5} M, pH 11, I 10^{-2} M), incubated with 470 nm particles (0.1%, pH 7, I 10^{-3} M), rinsed 6 times with water and dried with a nitrogen flow. The adhering particles were under the form of aggregates, usually bidimensional along the surface plane, sometimes tridimensional (i.e. forming multilayers). Attempts were made to improve the homogeneity of the colloidal particle distribution, keeping the colloidal particle treatment unchanged but using polycations which differ according to functional groups, hydrophobicity and size, and changing polycation treatment conditions : (i) PAH, PLL, PEI, IPDDA and hPDDA; 10^{-7} M at pH 3 and 10^{-5} M at pH 11; I 10^{-3} and 10^{-1} M; (ii) PAH and IPDDA; 10^{-7} and 10^{-5} M; pH 3, 7 and 11; I 10^{-3} , 10^{-2} and 10^{-1} M. In summary, polycation adsorption at pH 7 or 11 and low ionic strength (10^{-3} , 10^{-2} M) provided a higher degree of

coverage by colloidal particles; PAH was as efficient as, or better than other polymers tested; a polycation concentration of 10^{-5} M was more efficient than 10^{-7} M. However in all cases, the adhering particles were under the form of aggregates as described above.

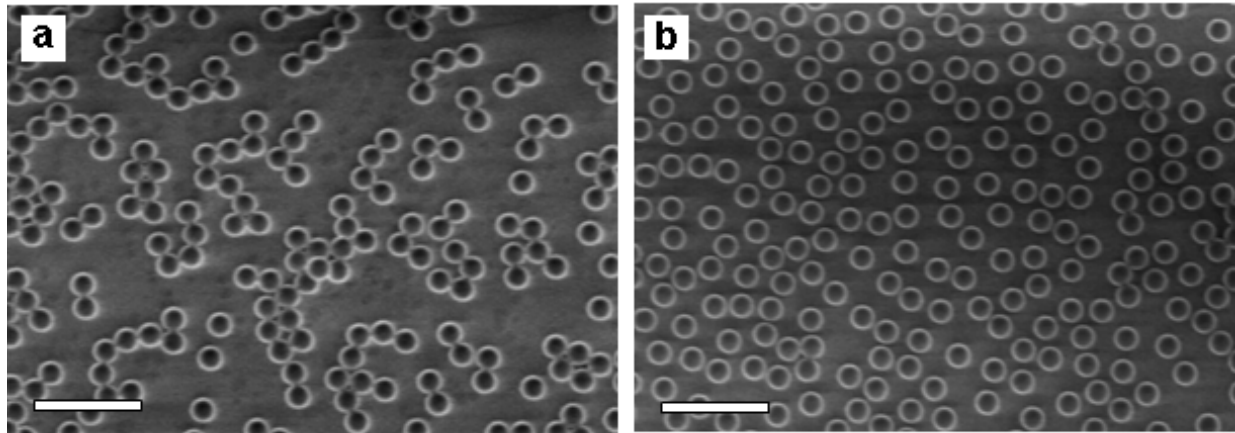


Fig. 4. SEM images obtained on PAH-conditioned (10^{-5} M, pH=11, $I=10^{-2}$ M) glass samples, submitted to latex particle adhesion (470 nm in diameter, 0.1%, pH=7, $I=10^{-3}$ M), rinsed with water and dried under a gentle nitrogen flow (a) or rinsed with water, then with isopropanol and air-dried (b). Scale bars: 2 μ m.

A more homogeneous particle distribution was obtained when the sample was rinsed first with water then with isopropanol and left to dry in air overnight, as shown in Figure 4b. Both images of Figure 4 present the same degree of particle coverage ($\sim 40\%$), but in image b, no aggregation is present and the particle distribution is more random. The influence of rinsing and drying procedures on the layer of latex particles may be due to their gathering together by the movement of the liquid film or by the nitrogen flow. In order to avoid particle aggregation at high coverage, Hanarp et al. (2001) attempted to retain particles in place during drying by adsorbing smaller silica particles between the latex particles or by heating the samples with adhering particles in boiling water in order to deform the particles and increase the contact area with the substrate. In the present work, rinsing with isopropanol was found to be efficient (Figure 4b); this is attributed to the reduction of capillary forces owing to the 3 times lower surface tension of isopropanol compared to water ((21.7 mN/m compared to 73.0 mN/m (Weast, 1972)).

Particle adhesion was further studied using substrates conditioned with PAH as described above, rinsing 3 times with water and 3 times with isopropanol, followed by air drying. Figure 5 presents representative results obtained by incubating the conditioned substrate during 2 hours with the colloids at 0.1 % concentration, using 3 pH values and 2 ionic strengths. At pH 7 with a low ionic strength and at pH 11, substrates were covered by a homogeneous layer of particles. In contrast, a high degree of aggregation was observed at pH 3 whatever the ionic strength, and at pH 7 with a high ionic strength.

Figure 6 (a, b) presents micrographs obtained after adhesion of the two kinds of latex particles separately (470 nm or 65 nm; 0.1%, pH 7, $I=10^{-3}$ M), with isopropanol rinsing and air drying. Two counting methods were used in order to assess the degree of substrate coverage. Binarization and automatic processing of SEM images allow counting to be made more rapidly and on a large number of images in comparison with manual counting.

However, it involves operations which could possibly create systematic variations. Binarization of SEM images gave degrees of coverage of $50.2 \pm 5 \%$ and $14.6 \pm 4 \%$ on surfaces layered with 470 and 65 nm particles, respectively. A consistent degree of substrate coverage was obtained using manual counting (470 nm : $45.2 \pm 2 \%$; 65 nm : $10.7 \pm 1 \%$). The differences between the two modes of counting were thus in the range of the standard deviation. Samples with adherent particles were also analyzed by XPS (Table 1). For samples 7 and 8, 470 nm particles were used and the degree of coverage was 53 and 27 %, respectively; for sample 9, 65 nm particles were used and the degree of coverage was 15 %, as assessed by SEM image analysis. As compared with PAH conditioned substrates with no adhering latex, these three samples gave a higher concentration of carbon, a lower concentration of silicon, oxygen and nitrogen and indicated the presence of sulfur, characterized by a S 2p peak (showing the $2p_{3/2}$ and $2p_{1/2}$ components with S $2p_{3/2}$ observed at 169 eV), characteristic of sulfate and due to the latex surface.

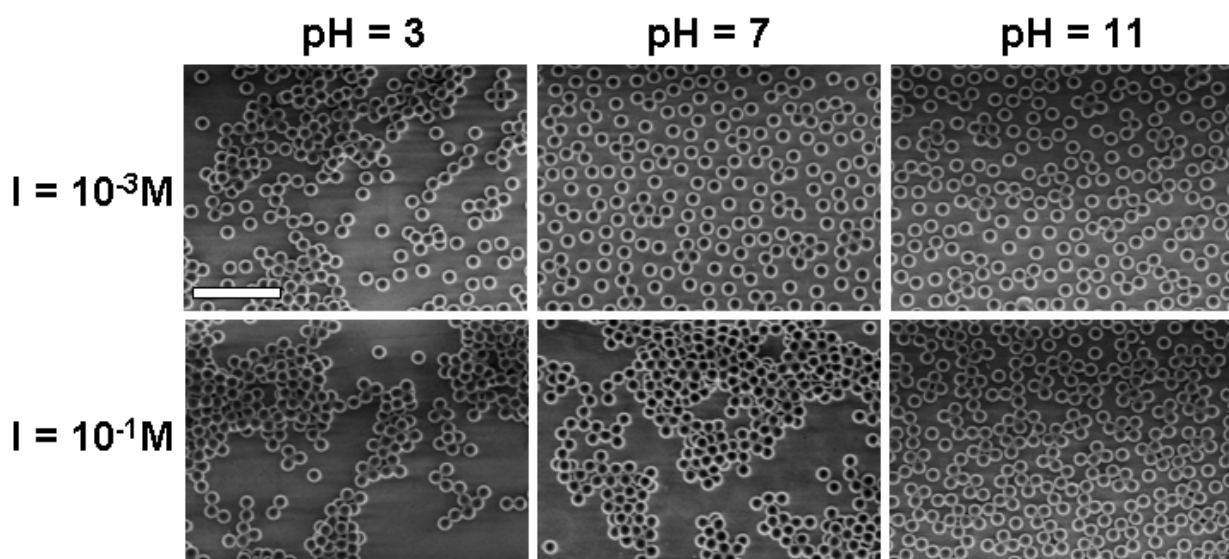


Fig. 5. SEM images obtained on PAH-conditioned (10^{-5}M , $\text{pH}=11$, $I=10^{-2}\text{M}$) glass samples, submitted to latex particle adhesion in different conditions of pH and ionic strength (470 nm in diameter particles, 0.1%), rinsed with water, then with isopropanol and air dried. Scale bars: 2 μm .

A variation of the duration of incubation of the PAH-conditioned substrate with the 470 nm latex (1 to 6 hours, 1 to 6 days) showed that an incubation time of at least 2 hours was required in order to obtain these degrees of coverage. However no increase of coverage was obtained when incubating for longer periods of times. Using a 1 % latex concentration instead of 0.1 % did not provide any rise of the degree of coverage (data not shown).

Obtaining a layer of adhering particles deserves discussion, considering not only interfacial interactions but also the amount of colloidal particles involved and mass transfer. Table 2 presents data computed for the experimental conditions of the treatments with 0.1 % colloidal suspensions. Similar data for PAH 10^{-5}M solution are given for comparison, considering the polycation as a non hydrated sphere of 3.0 nm radius; note that the hydrodynamic radius at pH 7.4 is about 5 times larger (Adamczyk et al., 2006).

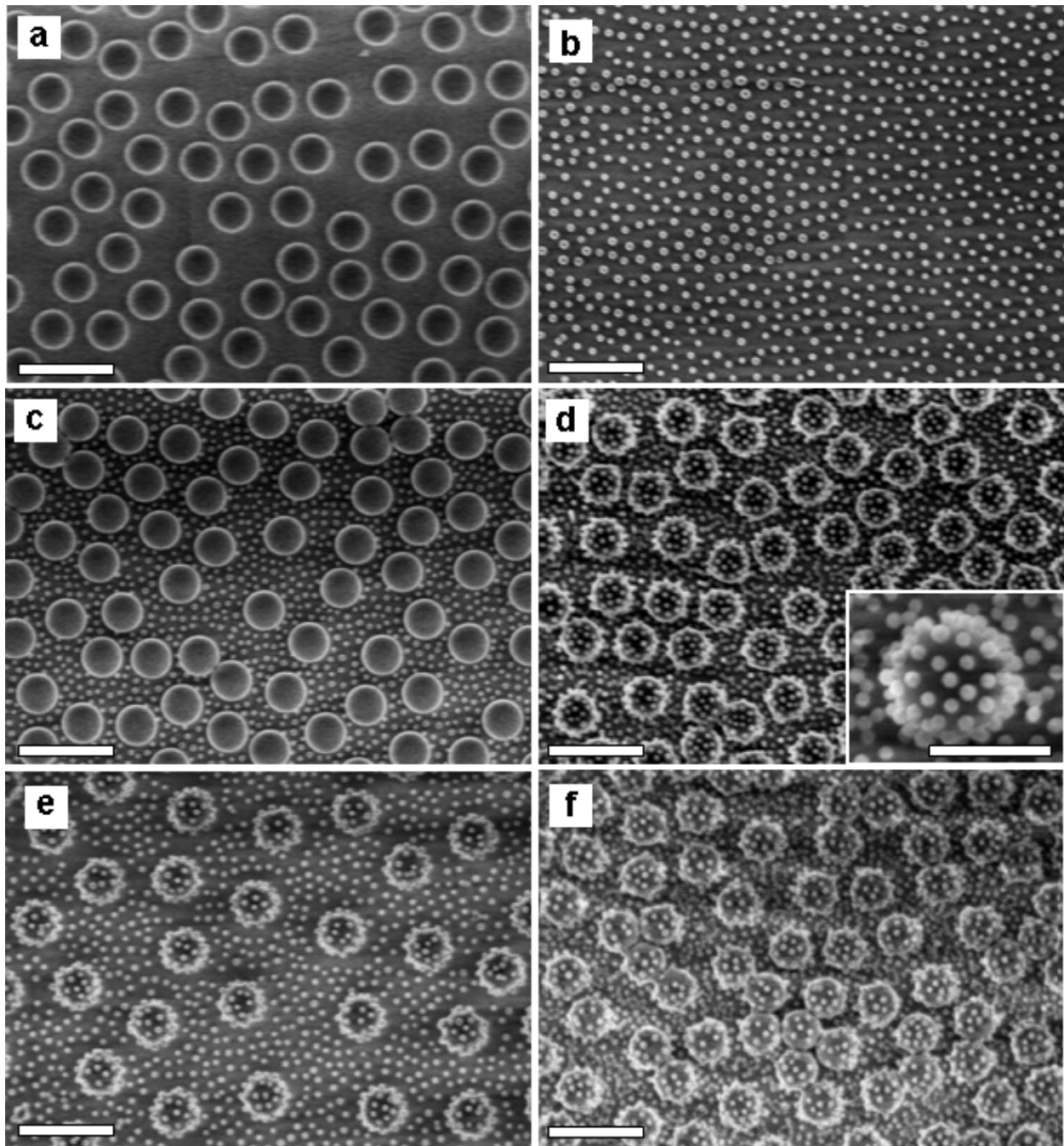


Fig. 6. SEM images obtained on PAH-conditioned (10^{-5}M , $\text{pH}=11$, $I=10^{-2}\text{M}$) glass samples, submitted to adhesion of latex particles (0.1% , $\text{pH}=7$, $I=10^{-3}\text{M}$, rinsing with water then with isopropanol) with 470 nm (a) and 65 nm diameter (b), and submitted to sequential adhesion of 470 nm and 65 nm particles without (c, bimodal I roughness) and with (d, e, f, bimodal II roughness) PAH adsorption after adhesion of the 470 nm particles. Image f was obtained on a sample prepared in the same experimental set as d, then submitted to immersion in PBS at 37°C for 24h . Images d and e were obtained on samples fabricated independently. The inset shows an enlargement of structures present on surfaces with bimodal II roughness. Scale bars: $1\ \mu\text{m}$. Scale bar inset: 500 nm .

- Area A occupied per particle in hexagonal close packing ($3.46 a^2$, a being the particle radius).
- Amount Q of particles required to cover the surface with a monolayer in hexagonal close packing.
- Concentration C of particles in the liquid phase, which, if expressed in ml^{-1} , is also the amount of particles involved in the preparation.
- Thickness e of the liquid layer containing the amount of particles required to make a monolayer.
- Diffusion coefficient D of the particles ($D = kT / 6\pi\eta a$), where k , T and η are the Boltzmann constant, the temperature and the viscosity, respectively.
- Time t_d required to produce a monolayer if the rate of adsorption is entirely controlled by diffusion through a concentration gradient created by adsorption itself (Crank, 1957): $t_d = \pi Q^2 / 4 C^2 D$.

It appears that the particles are in large excess of what is needed to make a monolayer. Mass transport by diffusion is fast for polycations and 65 nm latex particles. In contrast, a period of one day is expected to be needed for insuring the formation of a monolayer of 470 nm particles if diffusion is the rate controlling process. Thus sedimentation or convection should contribute to bringing the 470 nm particles to the surface. Considering a density of 1.05 g/cm^3 , the rate of sedimentation v_s of 470 nm particles is about 6.0 nm/s according to Stokes law. Accordingly the time t_s required to produce a monolayer if the rate is entirely controlled by sedimentation is $t_s = e / v_s = 13 \text{ hours}$. Actually the amount of adhering 470 nm particles does not increase significantly if the incubation time is extended from 1 hour to 6 days, suggesting that convection due to manipulation insures mass transport. The data of Table 2 also help to figure out in what limits it would be possible to control the adsorption of polycations and small latex particles by playing with incubation time and concentration.

	PAH 10⁻⁵ M	Latex 65 0.1 %	Latex 470 0.1 %
$A \text{ (nm}^2 \text{ part}^{-1}\text{)}$	32	$3.7 \cdot 10^3$	$1.91 \cdot 10^5$
$Q \text{ (part. cm}^{-2}\text{)}$	$3.1 \cdot 10^{12}$	$2.7 \cdot 10^{10}$	$5.2 \cdot 10^8$
$C \text{ (part. cm}^{-3}\text{)}$	$6.0 \cdot 10^{15}$	$7.0 \cdot 10^{12}$	$1.8 \cdot 10^{10}$
$e \text{ (}\mu\text{m)}$	5.2	39	284
$D \text{ (cm}^2\text{s}^{-1}\text{)}$	$7.2 \cdot 10^{-7}$	$6.7 \cdot 10^{-8}$	$9.3 \cdot 10^{-9}$
t_d	0.29 s	2.9 min	19 hours

Table 2. Particle characteristics relevant to experimental conditions. See text for details.

While mass transport is not a limiting factor for adhesion of 65 nm particles, the density of the monolayer remains fairly low (10 to 15 % degree of coverage). For this latex at the ionic strength of 10^{-2} M , the product ka , where κ is the inverse of the Debye length, is about 10. For this ka value, maximum coverages of about 35 % were reported for positively charged latex particles on mica (Johnson and Lenhoff, 1996) and for negatively charged latex particles on titanium oxide modified by successive adsorption of PDDA, polystyrene sulfonate and aluminium chloride hydroxide (Hanarp et al., 2001), in agreement with predictions based on repulsion between the particles considered as hard spheres. It is thus reasonable to consider that the coverage by the 65 nm latex is controlled by double layer

repulsion between particles. For this latex, a surface coverage of 10 to 15 % corresponds to an apparent area of $37 \cdot 10^3$ to $24 \cdot 10^3$ nm²/ particle, corresponding to an occupational diameter of 207 to 166 nm. The difference (142 to 101 nm) with the real particle size is larger than the latter, which demonstrates that the degree of coverage is limited by particle-particle repulsion.

If the particles were in hexagonal close packing, the area occupied per particle would be as presented in Table 2. A surface coverage of 45 % for the 470 nm latex thus corresponds to an apparent area per particle of $4.2 \cdot 10^5$ nm² and an occupational diameter of 700 nm. The difference of 230 nm between the occupational diameter and particle size is lower than the real particle diameter. Accordingly the degree of coverage is limited by the space available, considering a random distribution of particles. Consequently, the degree of coverage would be limited by the space available for 470 nm particles and by electrostatic repulsion for the 65 nm latex. Hanarp (2003) used the ionic strength (10^{-5} to 10^{-2} M), to control the density of 110 nm polystyrene particles adhering on titanium oxide conditioned with a solution of aluminium chloride hydroxide. Our data indicate that this method would not work for particles above 200 nm diameter.

Figure 5 shows aggregation of 470 nm particles when using a 10^{-1} M ionic strength at pH 3 or 7, or when using a 10^{-3} M ionic strength at pH 3. The surface charge of colloids used here is not affected by pH as confirmed by Schulz et al. (1994a, 1994b), who used latex particles of 131 nm from the same provider and with the same surface specifications as the particles used here. If the aggregates were formed in the suspension, the adhering amount would be expected to increase with time in the range of a few hours or when increasing the concentration from 0.1 to 1 %, in contrast with observations. This suggests that aggregation may take place at the sol - substrate interface owing to low particle - particle repulsion, in addition to the tendency to gather together induced by subsequent solvent evaporation. The aggregation may also be favored by partial desorption of the polycation, as it is enhanced at a pH 3 and 7, at which the polycation is more highly charged (Choi and Rubner, 2005).

3.3 Nanostructured surfaces with bimodal roughness

Surfaces with bimodal I roughness (Figure 6c) were created by adding 65 nm particles subsequently to the 470 nm particles (cf Figure 1c,d). The degree of substrate coverage with 470 nm particles was of 46.9 ± 1 % on this sample. This approach is similar to that of Takeshita et al. (2004) using poly(ethylene terephthalate) conditioned with PAH and adhesion of 350 nm carboxylated polystyrene latex particles followed by 100 nm particles. However, the layer obtained in that case was not regular, despite sonication of the solution to prevent latex aggregation. We attribute this to the fact that the samples were rinsed with water before drying.

Surfaces with bimodal II roughness (Figure 6d) were prepared by adsorbing PAH after the formation of the first adhering layer (cf Figure 1b,c,e,f). In this way, 65 nm particles were adhering not only to the glass substrate but also to the 470 nm particles, providing raspberry-like structures. This procedure was repeated five times independently and 3 to 15 samples were prepared in each experiment, demonstrating the repeatability as well as the reproducibility of the method. Figure 6 (d, e) presents the extreme results obtained, corresponding to degrees of coverage by 470 nm particles of 50 ± 3 % and 22 ± 1 %, respectively.

Owing to the possible interest of nanostructured surfaces in the field of biointerfaces, samples with adhering particles were incubated in phosphate buffer saline (the main constituent of culture media) for 24 h at 37°C, followed by rinsing with water, rinsing with isopropanol and drying. The result obtained with a bimodal II roughness is presented in Figure 6f. The observed morphology is similar to that of the sample not exposed to buffer (Figure 6d), demonstrating the robustness of the protocol and of the nanostructured surface obtained.

Recently published works aimed at creating this kind of roughness using different approaches. Suspensions of raspberry-like particles were prepared by styrene polymerization on silica particles (Perro et al., 2006; Reculosa et al., 2002). In another study, silica particles having different sizes and bearing functional groups were firstly synthesized independently and then mixed to react together. The obtained aggregates were then grafted on a specific substrate to obtain a dual-size roughness surface (Xiu et al., 2006). In another approach, a layer of silica particles in hexagonal close packing was created on a substrate, and gold nanoparticles were formed on the top of the silica spheres by sputtering (Ming et al., 2005). The method used in the present work has several advantages, such as the use of components which are commercially available (polycation, latex particles), and a simple procedure (sequential steps of polycation adsorption and colloid adhesion) which does not require sophisticated devices or complex reactions. The protocol could be extended to other particle sizes for obtaining a broader panel of roughness, the density of the two types of particles could be tuned, and architectures could be elaborated with more than two particle sizes. The bimodal surfaces of type II roughness mimic the particular topography observed on Lotus leaf. A superhydrophobic surface is thus expected to be obtained after treatment with compounds conferring a low surface energy (Bravo et al., 2007).

4. Conclusion

Nanostructured surfaces were fabricated through assembly of PAH and polystyrene latex particles. Thereby, different types of roughness were created, with a single layer of particles (65 or 470 nm), a layer of two types of particles (65 and 470 nm) - bimodal roughness of type I - or a layer of raspberry-like relief features (65 nm on 470 nm) - bimodal roughness of type II. The best conditions for glass conditioning by PAH were a high pH (11) and a low ionic strength (10^{-2} M). A neutral or alkaline pH with a low ionic strength was satisfactory for the adhesion of the colloidal particles on PAH-conditioned glass. Terminating the rinsing procedure with isopropanol before air drying was needed to avoid particle aggregation due to capillary forces. Incubation in PBS, a buffer solution mimicking the electrolyte composition of biological fluids, did not alter the structures obtained.

After PAH conditioning, the thickness of the adsorbed layer detected on glass was in the range of 2.5 to 3.5 nm ; this layer contained an appreciable amount of adventitious organic contaminants. The degree of ionization of PAH at the outermost part of the adsorbed layer was low and did not provoke a surface charge reversal. This indicates that the colloid particles were not attracted by long distance forces but rather suggests a change of PAH protonation with a redistribution of counterions when colloidal particles approached the PAH-modified glass.

The control of the degree of coverage by adhering particles for performing colloidal lithography may be pursued by playing with interfacial interactions, and thus with pH and ionic strength. On the other hand it may be pursued by playing with mass transfer:

substrate orientation (upward, downward, vertical), convection, particle concentration and contact time. The selection of the best approach depends primarily on the particle size, which is critical in the range of 100 nm, and secondarily on particle density and on the desired degree of coverage.

5. Acknowledgements

The support of the Foundation for Training in Industrial and Agricultural Research (FRIA), of the Belgian National Foundation for Scientific Research (FNRS), of the Région Wallonne and of the Federal Office for Scientific, Technical and Cultural Affairs (Interuniversity Poles of Attraction Program) is gratefully acknowledged.

6. References

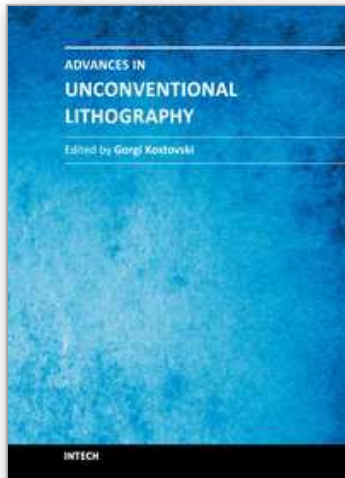
- Adamczyk, Z., Zembala, M., & Michna, A. (2006). Polyelectrolyte adsorption layers studied by streaming potential and particle deposition. *J. Colloid Interface Sci.*, 303, 353-364
- Adamczyk, Z., Zembala, M., Kolasinska, M., & Warszynski, P. (2007) Characterization of polyelectrolyte multilayers on mica and oxidized titanium by steaming potential and wetting angle measurements. *Colloid Surf. A: Physicochem. Eng. Asp.*, 302, 455-460
- Agheli, H., Malmstrom, J., Hanarp, P., & Sutherland, D.S. (2006). Nanostructured biointerfaces. *Mater. Sci. Eng. C: Biomimetic Supramol. Syst.*, 26, 911-917
- Barthlott, W., & Neinhuis C. (1997). Purity of the sacred lotus, or escape from contamination in biological surfaces. *Planta*, 202, 1-8
- Bertrand, P., Jonas, A., Laschewsky, A., & Legras R. (2000). Ultrathin polymer coatings by complexation of polyelectrolytes at interfaces: Suitable materials, structure and properties. *Macromol. Rapid Commun.*, 21, 319-348.
- Boonaert, C.J.P., Dupont-Gillain, C.C., Dengis, P.B., Dufrêne Y.F., & Rouxhet, P.G. (1999). Cell separation, flocculation, In: *Encyclopedia of bioprocess technology: Fermentation, biocatalysis, and bioseparation*, M.C. Flickinger, S.W. Drew (Eds.), pp. 531-548, John Wiley & Sons, Inc., New York
- Boonaert, C.J.P., Dufrêne, Y.F., & Rouxhet, P.G. (2002). Adhesion (primary) of microorganisms onto surfaces, In: *Encyclopedia of environmental microbiology*, G. Bitton (Ed.), pp. 113-132, John Wiley & Sons Inc., New York
- Bravo, J., Zhai, L., Wu, Z., Cohen, R.E., & Rubner M.F. (2007). Transparent superhydrophobic films based on silica nanoparticles. *Langmuir*, 23, 7293-7298
- Caillou, S., Gerin, P.A., Nonckreman, C.J., Fleith, S., Dupont-Gillain, C.C., Landoulsi, J., Pancera, S.M., Genet, M.J., & Rouxhet, P.G. (2008). Enzymes at solid surfaces: nature of the interfaces and physico-chemical processes. *Electrochim. Acta*, 54, 116-122
- Changui, C., Doren, A., Stone, W.E.E., Mozes, N., & Rouxhet, P.G. (1987). Surface properties of polycarbonate and promotion of yeast cell adhesion. *Journal de Chimie Physique et de Physico-Chimie Biologique*, 84, 275-281
- Chen, K.M., Jiang, X., Kimerling, L.C., & Hammond, P.T. (2000). Selective self-organization of colloids on patterned polyelectrolyte templates. *Langmuir*, 16, 7825-7834

- Choi, J., & Rubner, M.F. (2005). Influence of the degree of ionization on weak polyelectrolyte multilayer assembly. *Macromolecules*, 38, 116-124
- Claesson, P.M., Poptoshev, E., Blomberg, E., & Dedinaite, A. (2005). Polyelectrolyte-mediated surface interactions. *Adv. Colloid Interface Sci.*, 114-115, 173-187
- Crank, J. (1957). *The mathematics of diffusion*, Oxford University Press, p. 30-31
- Davies, R.J., Dix, L.R., & Toprakcioglu C. (1989). Adsorption of poly-L-lysine to mica powder. *J. Colloid Interface Sci.*, 129, 145-152
- Decher, G., & Hong, J.D. (1991). Build up of ultrathin multilayer films by a self-assembly process: Consecutive adsorption of anionic and cationic bipolar amphiphiles on charged surfaces. *Macromol. Chem. Macromol. Symp.*, 46, 321-327
- Dekeyser, C.M., Biltresse, S., Marchand-Brynaert, J., Rouxhet, P.G., & Dupont-Gillain, C.C. (2004). Submicrometer-scale heterogeneous surfaces by PS-PMMA demixing. *Polymer*, 45, 2211-2219
- Denis, F.A., Hanarp, P., Sutherland, D.S., & Dufrene, Y.F. (2002). Fabrication of nanostructured polymer surfaces using colloidal lithography and spin-coating. *Nano Lett.*, 2, 1419-1425
- Elgersma, A.V., Zsom, R.L.J., Lyklema, J., & Norde, W. (1992). Kinetics of single and competitive protein adsorption studied by reflectometry and streaming potential measurements. *Colloid Surf.*, 65, 17-28
- Fustin, C.A., Glasser, G., Spiess, H.W., & Jonas, U. (2004). Parameters influencing the templated growth of colloidal crystals on chemically patterned surfaces. *Langmuir*, 20, 9114-9123
- Gerin, P.A., Dengis, P.B., & Rouxhet, P.G. (1995). Performance of XPS analysis of model biochemical compounds. *Journal de Chimie Physique*, 92, 1043-1065
- Hanarp, P., Sutherland, D.S., Gold, J., & Kasemo B. (2001). Influence of polydispersity on adsorption of nanoparticles. *J. Colloid Interface Sci.*, 241, 26-31
- Hanarp, P., Sutherland, D.S., Gold, J., & Kasemo, B. (2003). Control of nanoparticle film structure for colloidal lithography. *Colloid Surf. A: Physicochem. Eng. Asp.*, 214, 23-36.
- Johnson, C.A., & Lenhoff, A.M. (1996). Adsorption of Charged Latex Particles on Mica Studied by Atomic Force Microscopy. *J. Colloid Interface Sci.*, 179, 587-599
- Lafuma, F. (1996). Mechanisms of flocculation and stabilisation of suspensions by organic polymers, In: *Paper Chemistry*, J.C. Roberts (Ed.), Chapman & Hall, London
- Li, J., Luan, S., Huang, W., & Han, Y. (2007). Colloidal crystal heterostructures by a two-step vertical deposition method. *Colloid Surf. A: Physicochem. Eng. Asp.* 295, 107-112
- Li, Z., Ravaine, V., Ravaine, S., Garrigue, P., & Kuhn, A. (2007). Raspberry-like gold microspheres: preparation and electrochemical characterization. *Adv. Functional Materials*, 17, 618-622
- Lindquist, G.M., & Stratton, R.A. (1976). The role of polyelectrolyte charge density and molecular weight on the adsorption and flocculation of colloidal silica with polyethylenimine. *J. Colloid Interface Sci.*, 55, 45-59
- Meszaros, R., Varga, I., & Gilanyi, T. (2004). Adsorption of poly(ethyleneimine) on silica surfaces: Effect of pH on the reversibility of adsorption. *Langmuir*, 20, 5026-5029
- Ming, W., Wu, D., van Benthem, R., & de With, G. (2005). Superhydrophobic films from raspberry-like particles. *Nano Lett.*, 5, 2298-2301

- Nonckreman, C.J., Fleith, S., Rouxhet, P.G., & Dupont-Gillain, C.C. (2010). Competitive adsorption of fibrinogen and albumin and blood platelet adhesion on surfaces modified with nanoparticles and/or PEO. *Colloids and Surfaces B: Biointerfaces*, 77, 139-149
- Patankar, N.A. (2004). Mimicking the Lotus Effect: Influence of double roughness structures and slender pillars. *Langmuir*, 20, 8209-8213
- Perro, A., Reculosa, S., Bourgeat-Lami, E., Duguet, E., & Ravaine, S. (2006). Synthesis of hybrid colloidal particles: From snowman-like to raspberry-like morphologies. *Colloid Surf. A: Physicochem. Eng. Asp.*, 284-285, 78-83
- Petrov, A.I., Antipov, A.A., & Sukhorukov, G.B. (2003). Base-acid equilibria in polyelectrolyte systems: From weak polyelectrolytes to interpolyelectrolytes complexes and multilayered polyelectrolyte shells. *Macromolecules*, 36, 10079-10086.
- Reculosa, S., Poncet-Legrand, C., Ravaine, S., Mingotaud, C., Duguet, E., & Bourgeat-Lami, E. (2002). Syntheses of raspberry-like silica/polystyrene materials. *Chem. Mater.*, 14, 2354-2359
- Roberts, J.C. (1996). The surface chemistry of paper and the paper-making system, In: *The Chemistry of Paper*, J.C. Roberts (Ed.), The Royal Society of Chemistry, Letchworth.
- Rouxhet, P.G., Doren, A., Dewez, J.L., & Heuschling, O. (1993). Chemical composition and physico-chemical properties of polymer surfaces. *Prog. Org. Coat.*, 22, 327-344
- Schaak, R.E., Cable, R.E., Leonard, B.M., & Norris, B.C. (2004). Colloidal crystal microarrays and two-dimensional superstructures: a versatile approach for patterned surface assembly. *Langmuir*, 20, 7293-7297
- Schulz, S.F., & Sticher, H. (1994a). Surface charge densities and electrophoretic mobilities of aqueous colloidal suspensions of latex spheres with different ionizable groups. *Prog. Colloid Polym. Sci.*, 97, 85-88
- Schulz, S.F., Gisler, T., Borkovec, M., & Sticher, H. (1994b). Surface charge on functionalized latex spheres in aqueous colloidal suspensions. *J. Colloid Interface Sci.*, 164, 88-98
- Tagliazucchi, M., Calvo, E.J., & Szleifer, I. (2008). Redox and acid-base coupling in ultrathin polyelectrolyte films. *Langmuir*, 24, 2869-2877
- Takeshita, N., Paradis, L.A., Oener, D., McCarthy, T.J., & Chen, W. (2004). Simultaneous tailoring of surface topography and chemical structure for controlled wettability. *Langmuir*, 20, 8131-8136
- Tanuma, S., Powell, C.J., & Penn, D.R. (1997). Calculations of electron inelastic mean free paths (IMFPs). VI. Analysis of the Gries inelastic scattering model and predictive IMFP equation. *Surf. Interface Anal.*, 25, 25-35
- Van Haecht, J.L., Bolipombo, M., & Rouxhet, P.G. (1985). Immobilization of *Saccharomyces cerevisiae* by adhesion: treatment of the cells by aluminum ions. *Biotechnol. Bioeng.*, 27, 217-224
- Weast, R.C. (1972). *Handbook of Chemistry and Physics*, 52nd ed., The Chemical Rubber C.O., Cleveland.

- Wenzel, R.N. (1936). Resistance of solid surfaces to wetting by water. *J. Ind. Eng. Chem.*, 28, 988-994
- Wood, M.A. (2007). Colloidal lithography and current fabrication techniques producing in-plane nanotopography for biological applications. *J. R. Soc. Interface*, 4, 1-17
- Xiu, Y., Zhu, L., Hess, D.W., & Wong, C.P. (2006). Biomimetic creation of hierarchical surface structures by combining colloidal self-assembly and Au sputter deposition. *Langmuir*, 22, 9676-9681
- Yang S., Cai, W., Yang, J., & Zeng, H. (2009). General and simple route to micro/nanostructured hollow-sphere arrays based on electrophoresis of colloids induced by laser ablation in liquid. *Langmuir*, 25, 8287-9291

IntechOpen



Advances in Unconventional Lithography

Edited by Dr. Gorgi Kostovski

ISBN 978-953-307-607-2

Hard cover, 186 pages

Publisher InTech

Published online 09, November, 2011

Published in print edition November, 2011

The term Lithography encompasses a range of contemporary technologies for micro and nano scale fabrication. Originally driven by the evolution of the semiconductor industry, lithography has grown from its optical origins to demonstrate increasingly fine resolution and to permeate fields as diverse as photonics and biology. Today, greater flexibility and affordability are demanded from lithography more than ever before. Diverse needs across many disciplines have produced a multitude of innovative new lithography techniques. This book, which is the final instalment in a series of three, provides a compelling overview of some of the recent advances in lithography, as recounted by the researchers themselves. Topics discussed include nanoimprinting for plasmonic biosensing, soft lithography for neurobiology and stem cell differentiation, colloidal substrates for two-tier self-assembled nanostructures, tuneable diffractive elements using photochromic polymers, and extreme-UV lithography.

How to reference

In order to correctly reference this scholarly work, feel free to copy and paste the following:

Christine C. Dupont-Gillain, Cristèle J. Nonckreman, Yasmine Adriaensen and Paul G. Rouxhet (2011). Fabrication of Surfaces with Bimodal Roughness Through Polyelectrolyte/Colloid Assembly, *Advances in Unconventional Lithography*, Dr. Gorgi Kostovski (Ed.), ISBN: 978-953-307-607-2, InTech, Available from: <http://www.intechopen.com/books/advances-in-unconventional-lithography/fabrication-of-surfaces-with-bimodal-roughness-through-polyelectrolyte-colloid-assembly>

INTECH
open science | open minds

InTech Europe

University Campus STeP Ri
Slavka Krautzeka 83/A
51000 Rijeka, Croatia
Phone: +385 (51) 770 447
Fax: +385 (51) 686 166
www.intechopen.com

InTech China

Unit 405, Office Block, Hotel Equatorial Shanghai
No.65, Yan An Road (West), Shanghai, 200040, China
中国上海市延安西路65号上海国际贵都大饭店办公楼405单元
Phone: +86-21-62489820
Fax: +86-21-62489821

© 2011 The Author(s). Licensee IntechOpen. This is an open access article distributed under the terms of the [Creative Commons Attribution 3.0 License](#), which permits unrestricted use, distribution, and reproduction in any medium, provided the original work is properly cited.

IntechOpen

IntechOpen